



## Tribological effect of thermal energy on TIG arc surfacing techniques for surface modification of stainless steel

Alin Qistina Shamsuri <sup>1</sup>, Lailatul Harina Paijan <sup>1\*</sup>, Zulkifli Mohd Rosli <sup>2</sup>, Mohd Fauzi Mamat <sup>2</sup>

<sup>1</sup> Faculty of Industrial and Manufacturing Technology and Engineering, Universiti Teknikal Malaysia Melaka, Hang Tuah Jaya, 76100 Durian Tunggal, Melaka, MALAYSIA.

\*Corresponding author: lailatulharina@utem.edu.my

KEYWORDS	ABSTRACT
Tribological Thermal energy TIG arc surfacing Hardness Wear rate	TIG (tungsten inert gas) torch surface modification is a unique process that can produce the surface alloying on a work surface and effectively improve surface hardness while altering the tribological behaviors. The significance of this work is to examine the influence of thermal energy on the surface characteristic of 2205 duplex stainless steel samples. The thermal energy varied from 0.48 to 1.440 KJ/mm. The surface hardness and microstructure features of the tribological properties of the materials were examined. Results indicate that, as thermal energy increases, the hardness value increases, thereby resulting in an increase of tribological properties. However, at higher thermal energy of 1.440 KJ/mm, the modified surface exhibits cracking in the melt layer. The microstructure transformed into different populations of dendritic structures. The best thermal energy obtained was 0.768 KJ/mm that resulted in the lowest wear rate of $3.0 \times 10^{-4} \text{ mm}^3/\text{Nm}$ and friction coefficient of 0.43. High hardness of the surface modification and increased tribological behavior were linked to higher levels of arc energy during TIG melting process.

Received 29 July 2024; received in revised form 9 Nov 2024; accepted 12 February 2025.

To cite this article: Shamsuri et al., (2025). Tribological effect of thermal energy on TIG arc surfacing techniques for surface modification of stainless steel. Jurnal Tribologi 44, pp.53-66.

## 1.0 INTRODUCTION

Surface modification process changes the properties of the surface at the certain depth level of the substrate. Physical Vapor Deposition (PVD), and Chemical Vapor Deposition (CVD) are typical methods used to deposit a thin overlay (coatings) on the substrate in the range of 1-10  $\mu\text{m}$  and small interaction takes place on the substrate material (Yuvaraj, 2018; Kumar & Singh, 2024). Unlike TIG arc surfacing process, it can modify the surface layer and produce a thick surface composite layer; the layer thickness can range from hundreds of micrometers to several millimeters. This is contributing from the thermal energy supplied during the process resulting in deep penetration of the modified surface. TIG arc surfacing is an alternative technique for modifying the surface layer and fabrication of surface composites. The surface layer with this technique becomes more beneficial with the presence of ceramic particles deposited into the modified layer as conducted by previous researchers (Paraye et al., 2021; Bello et al., 2020; Idriss et al., 2021; Sahoo et al., 2018).

The effortless integration of surface modification techniques into every aspect of our lives will have a significant impact on sustainability, operational ability, and service life. Therefore, a wide variety of industrial operations benefit from coated surfaces in terms of cost efficiency and productivity. In addition, wear resistance can be strengthened by applying a variety of surface modification techniques. Surface modification can reduce the financial and time costs associated with developing new materials. It is also among the easiest and most efficient solutions for the wear issue with modern technology. The part's operating performance is determined by the changes of the microstructure that can improve tribological properties. A suitable single or combined strengthening technique is chosen based on the requirements to modify the surface layer's microstructure, surface performance, and extend the equipment's operational life (Ren et al., 2023; Subramaniam et al., 2021).

Thermal energy is a key factor that influences surface modification using welding and melting techniques. It affects the melting cooling rate and microstructure in the surface coating region, resulting in the quality level of the surface modification. Productivity could be increased, and the defects can be minimized appropriately by controlling thermal energy. Therefore, to ensure the quality and efficiency increased in surface modification process, a study into the influence mechanism and thermal energy control method is essential (Guo et al. 2023; Liu et al., 2023; Moi et al., 2019; Azwan et al. 2019; Amuda et al., 2011).

Furthermore, with the development of science and technology and the progress of industrial manufacturing, the requirements for high-quality, high-precision, and high-reliability welding processes are getting higher and higher. Therefore, it is of great implication to promote the development of welding technology and industries to optimize the surface modification using melting techniques and improve the surface quality of material and reliability of the process by studying the thermal input of TIG torch melting process (Paijan et al., 2024; Mamat et al. 2015; Adeleke et al., 2016).

Bharadwaj et al., 2022 demonstrated that the laser heat input played a vital role on the weld bead of Zr-2.5 wt.% Nb alloys in terms of penetration depth, top fusion and heat affected zone width. With increase in thermal energy from 312 to 800 J/mm, the penetration depth in Zr-2.5 wt.% Nb alloys increased from 2.5 mm to 4 mm. This work was conducted without the coating of the ceramic particles on the surface material. Other authors (Kumar et al., 2022) reported about the deposition of  $\text{TiB}_2$ -Fe coating developed on AISI 1020 steel by tungsten inert gas (TIG) cladding. The works revealed that at higher input, the larger melting depth of the coating due to dilution of the coating materials. At higher heat input of 800 J/mm, hard  $\text{TiB}_2$  transforms into

relatively soft TiB phases and decreases its hardness resulting in wear rate decreases. It shows that the lower heat input of 720 J/mm can produce the higher hardness of 3026 Hv compared to higher heat input. In contrast to the previous work by Paijan et al. 2018, revealed that the increment of thermal energy of 768 J/mm produced the higher hardness compared to thermal energy of 480 J/mm using the coating reinforcement of 20  $\mu\text{m}$  SiC ceramic particles. The increment of hardness is contributed from high population of fine dendrite and thin structure in the melt using thermal energy of 768 J/mm. The weight loss and coefficient friction were also reduced due to higher hardness produced in this sample. From all these contradicts results have occurred due to the different usage of ceramic particles, particle size and base material from the previous researchers.

Investigating the previous literature illustrates that the effect of various thermal energy on the surface modification with the deposition of silicon carbide particles size using TIG torch melting techniques has been less studied. In this regard, this research aims to investigate the TIG torch thermal energy of 0.48 KJ/mm, 0.768 KJ/mm and 1.440 KJ/mm incorporated with 60  $\mu\text{m}$  silicon carbide particles size was performed on duplex stainless steel (DSS). Then, the hardness, microstructure and wear resistance of the deposited coating containing silicon carbide fabricating via the TIG torch process were evaluated to determine the quality of the surface modification on DSS.

## 2.0 EXPERIMENTAL PROCEDURE

### 2.1 Materials and Ceramic Powder Deposition

For the development of surface modification, the powder of ceramic particles was pre-deposited on DSS surface (50 mm x 33 mm x 10 mm). The surface of the DSS was deoxidized by scrubbing with 220 grades SiC every paper and washed with acetone. The ceramic particles of silicon carbide powder with average size of 60  $\mu\text{m}$ , weighed with 0.5 mg/mm<sup>2</sup> were mixed with 5% polyvinyl acetate (PVA), 2 drops of alcohol and 2 drops of distilled water. After this step, a paste was prepared from this mixture. A uniform layer of the paste was applied on the cleaned surface of the substrate with a thickness of about 0.8 – 1.0 mm. Afterward, to remove the moisture from the powder, the specimens were heated in a furnace for 1 hour by maintaining at 80 °C temperature.

### 2.2 Fabrication of Surface Modified DSS

The ceramic particles pre-deposited specimens were autogenously under a TIG torch using a thermal energy rate ranging from 0.48 KJ/mm, 0.768 KJ/mm and 1.440 KJ/mm which corresponds to welding currents of 80 to 100A and welding speeds of 1.0 to 2.0 mm/s. This work was conducted to investigate the impact of thermal energy on the microstructural features and tribological properties of surface modified DSS. Using argon shielding and a direct current electrode with negative polarity, a flow rate of 15 L/min was employed. The majority of the melting thermal energy was transmitted into the workpiece by the electrode's negative polarity, which also limited electrode heating and reduced heat loss via the tungsten electrode. Figure 1 illustrates the representation of the TIG cladding arrangement and outline of the track shifting to obtain a large area coating with 50% overlapping for wear test. The surface modification was implemented at varying thermal input as shown in Table 1. Equation 1 is used to calculate the actual thermal energy of the workpiece.

$$\text{Thermal energy} = \frac{0.48 \times \text{Current (A)} \times \text{Voltage (V)}}{\text{Transverse speed (mm/s)}} \quad (1)$$

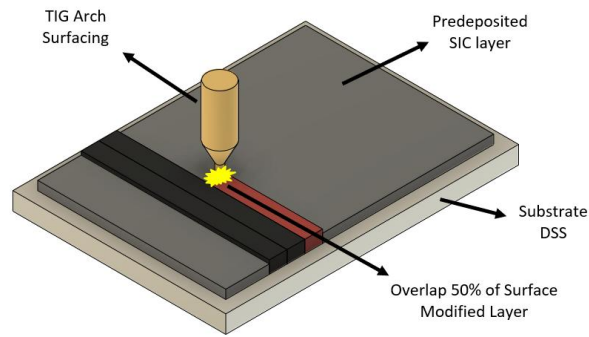


Figure 1: Schematic diagram of TIG cladding setup, and track shifting scheme to obtain a large area coating by 50% overlapping.

Table 1: Process parameter for various thermal energy of TIG arc surfacing techniques.

Sample	Current (A)	Voltage (V)	Travel Speed (mm/s)	Thermal input (KJ/mm)
1	100	20	2	0.48
2	80	40	2	0.768
3	100	30	1	1.440

### 2.3 Characterization and Vickers Micro Hardness Test of Surface Modified DSS

Using an EDM wire-cut machine, transverse portions of the surface modified DSS were cut to create specimens for microstructural investigation and micro-hardness testing. To get away from the residual layer and surface damage from the cut surface, the EDM machined specimens were first slightly ground using emery paper ranging from 400 to 1200 grit size. After that, the specimens were polished using 0.6  $\mu\text{m}$  alumina suspension paste until mirror finishes. Then, the polished specimens were etched in Kalling's reagent no. 2, a solution consisting of 100 ml ethanol, 100 ml HCL and 5-gram  $\text{CuCl}_2$ . To analyze the fine features of the microstructure transformation of surface modified DSS, the etched specimens were observed under a microscope using JEOL JSM 5600 scanning electron microscopy (SEM). The microstructure and thickness layer were captured to evaluate the performance of the surface modified DSS. Elemental analysis was conducted using EDX analyzer. Using a Wilson Welpert Vickers microhardness testing machine with a force load of 500 gf, pyramid diamond indenter and a dwell time of 10s, a longitudinal microhardness measurement was taken at positions 1 mm apart across the entire cross section of the modified layer.

## 2.5 Tribo-Testing Using Reciprocating Rig

A Ducom ball-on-disk tribometer was used to measure the wear of the surface modified layer in a room temperature. A surface modified surface specimen with dimension size of 15 mm × 15 mm was served as a disk and a 6 mm diameter alumina ceramic was employed as the ball. Within 10 minutes, the tests were run with a constant load of 30 N and frequency of 5 Hz according to ASTM D6079. The JEOL JSM 5600 SEM was used to study the worn marks of the modified surface DSS after tribo-testing.

## 3.0 RESULTS AND DISCUSSION

### 3.1 SEM Micrographs of Surface Modified DSS

The SiC ceramic particles with 60  $\mu\text{m}$  particle size are depicted in Figure 2. The microstructure was examined using X270 magnification SEM equipment. The different shapes of SiC ceramic particles are composed of hexagonal and cubic structures. The cross-sectional view of the surface modified layer for TIG arc surfacing processed with different thermal energy showed a hemispherical shape as shown in Figures 3 (a-c). The TIG arc surfacing for surface modification on DSS under thermal energy of 0.48 KJ/mm, 0.768 KJ/mm and 1.440 KJ/mm also produced a smooth surface without any significant defects. However, some crack was observed with thermal energy of 1.440 KJ/mm as shown in Figure 3(c). These cracks are likely to be caused by high fluidity melt and slow cooling. The viscous melt was unable to fill up the pores and thus produced porous regions. The escaping gas also left pores on the surface at the center region, but they easily compensated by less viscous melt in the surrounding vicinity. This explanation is supported in other investigations (Mridha, 2005).

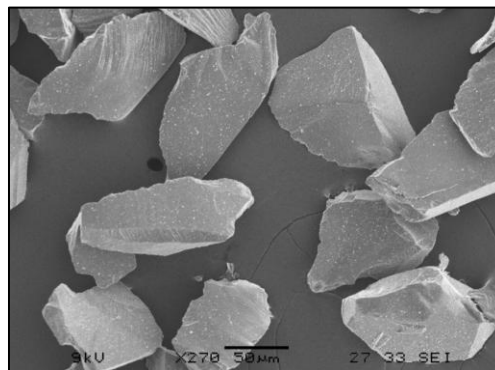


Figure 2: SEM microphotographs of SiC ceramic particles of 60  $\mu\text{m}$  at magnification of X270.

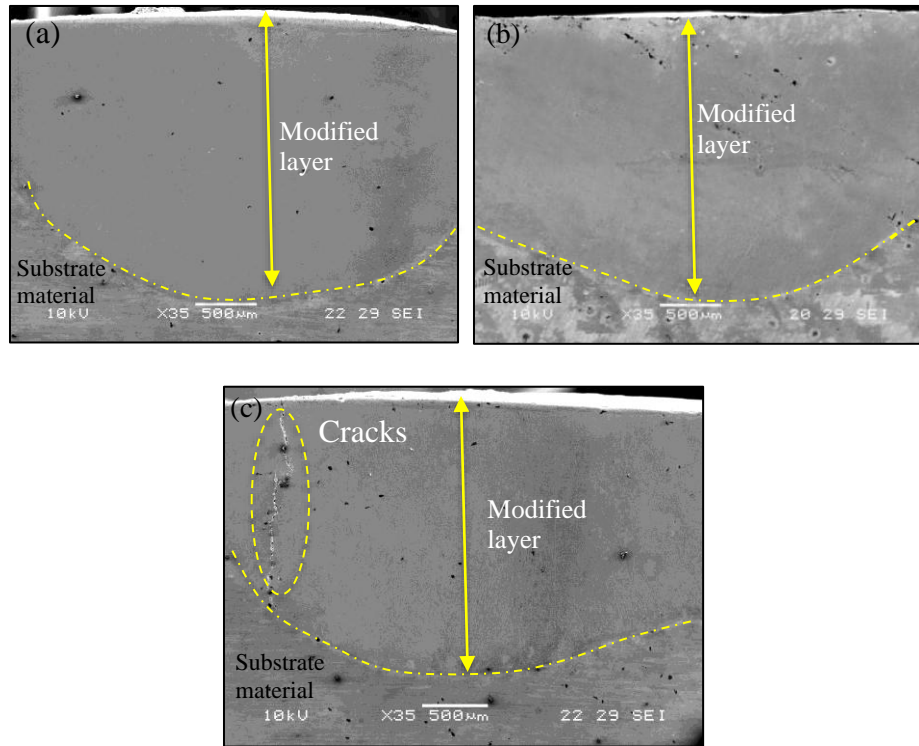


Figure 3: Cross sectional view of melt pool geometry of TIG surface modified DSS at different arc energy using (a) 0.48 KJ/mm, (b) 0.768 KJ/mm and (c) 1.440 KJ/mm.

Figures 4 (a-c) shows the SEM micrograph for surface modified DSS at different thermal energy of TIG arc surfacing. It can be seen that the microstructure exhibits a transformation into dendritic structure due to incorporation of partial and complete dissolved SiC in DSS surface layer. It was noted that as thermal energy increases the dendrite population in the surface modified layer also increases. The intensity of the thermal energy gives room for thin microstructure and therefore allows a slower cooling rate as the thermal input was amplified. Figure 4(b) shows the complete melting of SiC at 0.768 KJ/mm is the result of adequate heat input and high dilution between SiC and substrate DSS.

However, at the highest heat input of 1.440 KJ/mm as shown in Figure 4(c), the dendrite population becomes lesser and produces thick dendrite microstructure, which is in line with earlier research conducted by Bello et al. (2016). The sample took longer time to solidify because more SiC ceramic particles were dissolved in the melt pool when the sample melted at a higher heat input. This phenomenon is comparable to earlier research conducted by Adeleke & Maleque (2014). The melted layer's high fluidity encourages a stronger convection force, which may speed up the dissolution of the SiC ceramic particle and result in the formation of thicker dendritic microstructures. Based on this finding, it can be observed that thermal energy has a significant impact on the microstructure formation on the surface modified layer (Oleiwi & Jilabi, 2024).

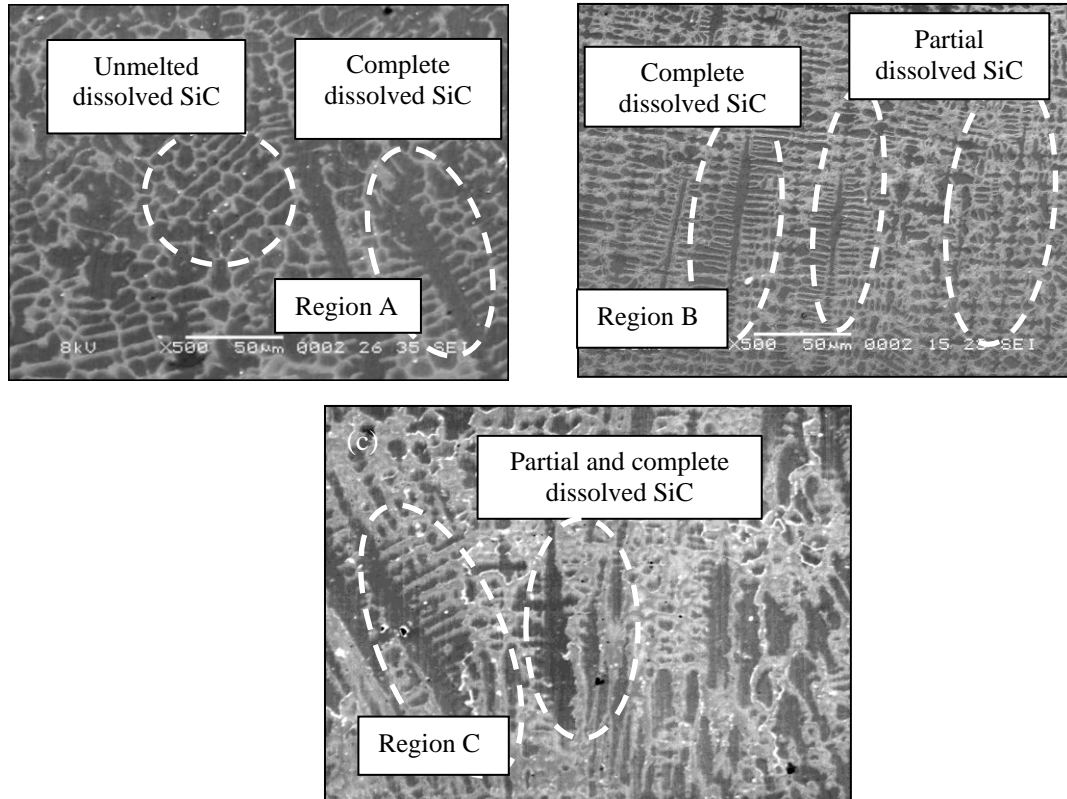


Figure 4: SEM Micrographs of TIG surface modified DSS at different arc energy using (a) 0.48 KJ/mm, (b) 0.768 KJ/mm and (c) 1.440 KJ/mm.

The EDX spectra for surface modified DSS at different thermal energy sources are shown in Figure 5. For lower heat input of 0.480 KJ/mm (region A in Figure 4a), it can be seen that the Si and C content obtained the percentage of 4.56 % and 7.93 %, respectively. Meanwhile, for higher heat input of 0.768 KJ/mm, the value was increased to 11.11% for Si and 13.24 % for C which was captured within dendritic structure at region B as shown in Figure 4(b). This phenomenon is due to the high concentration of dendritic structure at heat input of 0.768 KJ/mm which relates to the high amount of Si and C. At this heat input, the SiC is deposited well in the modified layer thus producing a high percentage of SiC. For higher heat input of 1.440 KJ/mm, the sample exhibited lower percentage of Si 5.66 % and C with 8.64% at region C in Figure 4 (c). This content reduction is contributed from the higher dissolution of SiC particulates in the modified layer using high arc energy thus producing a low percentage of SiC and lesser population of dendrite structure.

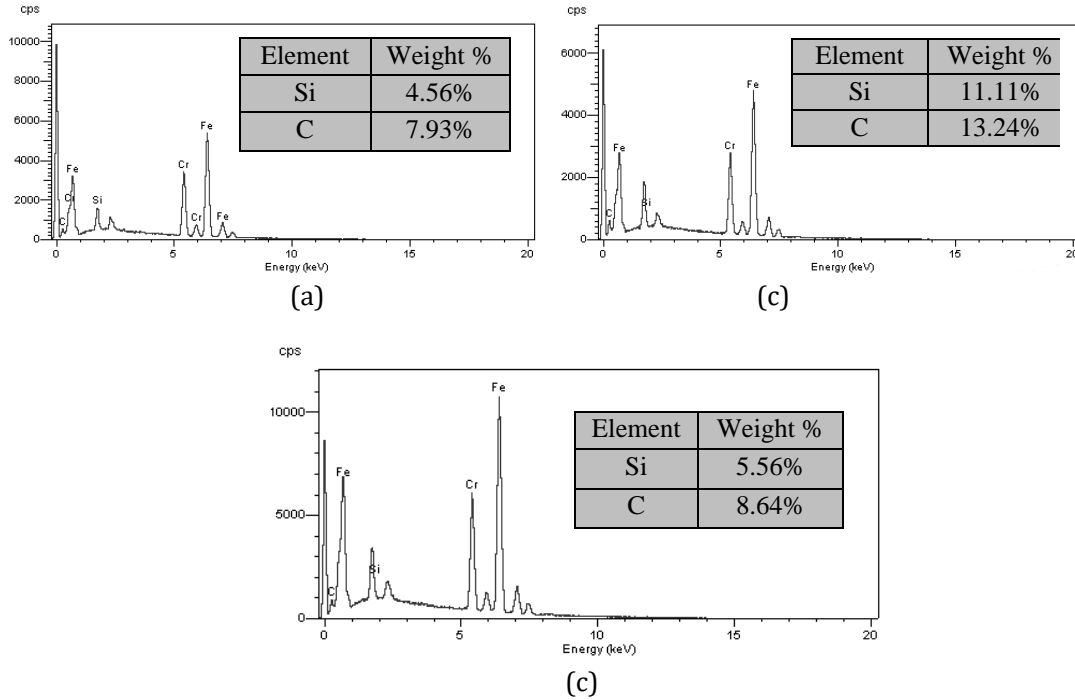


Figure 5: EDX spectra of TIG modified surface DSS within dendritic region as shown in Figure 4 indicating region A, B and C using thermal energy of (a) 0.48 KJ/mm, (b) 0.768 KJ/mm and (c) 1.440 KJ/mm.

### 3.2 Vickers Micro-Hardness Profile of Surface Modified DSS

To comprehend the disparity in the micro-hardness value at various locations of the surface modified DSS, and to understand the effect of thermal energy condition, the micro-hardness value was measured along the centerline of the modified layer. The hardness values were plotted concerning the distance from the top surface into the base metal, as depicted in Figure 6. For almost all thermal energy, the hardness increased gradually from the top surface towards the modified layer at distance between 100 and 250  $\mu\text{m}$  from the top surface. However, the hardness value reduced towards the substrate material. The decrease in hardness value at the bottom layer is attributed to a lower area fraction of SiC as compared to the top layer which also observed by previous researcher on mild steel through laser cladding (Muñoz-Escalona et al., 2020). Other than that, it can be observed that there is a substantial discrepancy in the hardness value for different thermal energy.



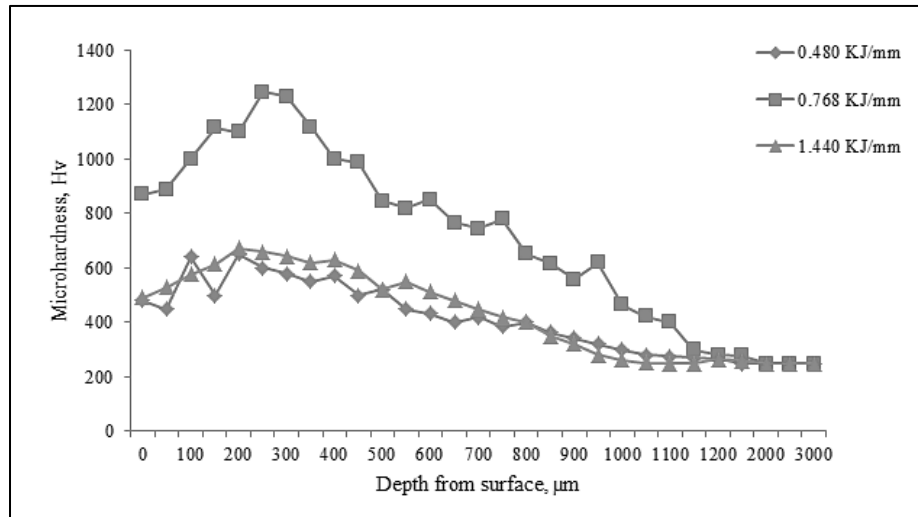


Figure 6: Micro-hardness variation along the depth of the surface modified DSS layer (measured at the center region of the cross-section) using thermal energy of (a) 0.48 KJ/mm, (b) 0.768 KJ/mm and (c) 1.440 KJ/mm.

Furthermore, the relatively higher hardness value of 1245 Hv was noted in the modified layer with thermal energy of 0.768 KJ/mm, and for increasing the thermal energy, the hardness value measured in the middle of the modified layer reduced significantly. This phenomenon also observed at the lower thermal energy of 0.48 KJ/mm. Correlating the hardness values with SEM micrographs of the modified layer revealed that for higher thermal input of 1.440 KJ/mm, the concentration of the SiC particles with the formation of dendrite structures in the modified layer is reasonably low, which resulted in a lower hardness value of 673.6 Hv. Almost all similar results also found for thermal energy of 0.48 KJ/mm whereby the hardness value reduced to 680.5 Hv. In contrast, it can be seen from the SEM micrographs that the higher concentration of the SiC particles using thermal energy of 0.768 KJ/mm leads to the highest value of hardness result. As witnessed from the microstructural analysis, it can be observed that the hardness value has strong correspondence to the presence of the SiC particles and dendrite population in the modified layer.

### 3.3 Tribological Properties on Wear Rate and Coefficient of Friction

The tribological properties of the surface modified DSS produced under various thermal energies were assessed through the tribometer equipment performed against alumina ceramic balls. Figure 7 demonstrates the wear characteristic (wear rate) and coefficient of friction (CoF) at thermal energy of 0.48 KJ/mm, 0.768 KJ/mm and 1.440 KJ/mm. The plots indicated that the wear rate is higher for sample fabricated under 0.48 KJ/mm and 1.440 KJ/mm compared to 0.768 KJ/mm. The variation in the wear properties for different thermal energy mainly attributed to a SiC particles concentration discrepancy in the microstructure of the surface modified DSS and corresponding disparity in their hardness properties as mentioned in Section 3.1 and 3.2.

It can be seen that the highest wear rate observed at sample fabricated under 0.48 KJ/mm with value of  $4.2 \times 10^{-4} \text{ mm}^3/\text{Nm}$  due to lower concentration of SiC particles in the sample and lower hardness value. This explanation is consistent with the findings of Mridha and Dyuti (2011), who discovered that mild steel produced reduced hardness and a smaller population of titanium

nitride structure with a lower heat input of 540 J/mm. However, the wear rate was reduced ( $3.0 \times 10^{-4} \text{ mm}^3/\text{Nm}$ ) at thermal energy of 0.768 KJ/mm and this is believed due to higher concentration of SiC particles and dendrite formation, also higher hardness in this sample. On the contrary, at higher thermal energy of 1.440 KJ/mm the wear rate increases with value of  $3.9 \times 10^{-4} \text{ mm}^3/\text{Nm}$ . and might be related to the lower concentration of dendrite structures and lower hardness value.

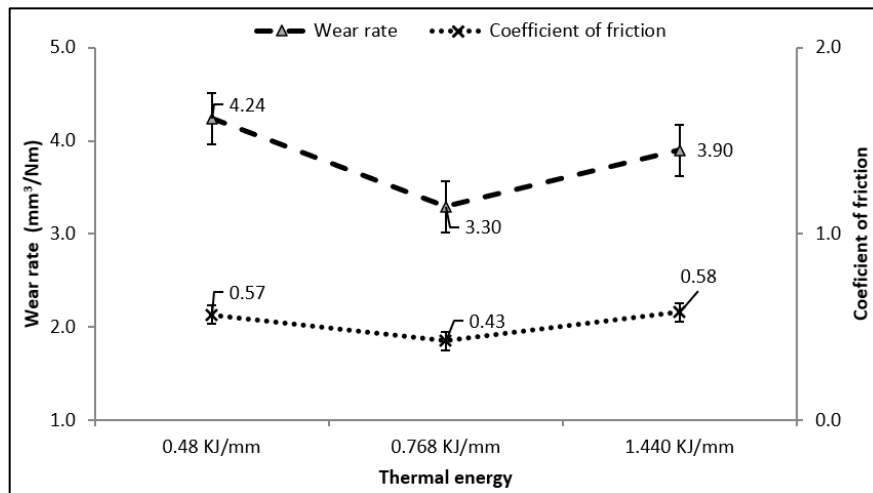


Figure 7: Wear rate and coefficient of friction for surface modified DSS fabricated at thermal input of 0. 480 KJ/mm, 0.768 KJ/mm and 1.440 KJ/mm.

The average CoF of surface modified DSS at different thermal energy sources has been shown and compared in Figure 7. At thermal energy of 0.48 KJ/mm, the higher CoF was obtained with CoF value of 0.57 which is due to lower concentration of dendrite and lower hardness obtained in samples. In contrast, a significant improvement of CoF was observed under the thermal energy of 0.768 KJ/mm. This phenomenon can be explained by the higher concentration of dendrites and higher hardness. This spectacle coincides with the finding by Adeleke & Maleque (2016) which described that the presence of TiC particles in titanium alloy had successfully reduced the CoF of the material due to enhancement of hardness values.

The obtained results proved the use of ceramic particles enhance the friction properties of the sample. When two surfaces come in contact with each other, the SiC particles prevent continuous contact. Other factors affecting CoF are the presence of ceramic particles with high thermal conductivity, which inhibits a significant rise in the instantaneous temperature during wear and, consequently, avoids an increase in the COF. A similar finding observed by Kheradmand et al. (2022), revealed that the copper particles act as a medium to prevent the increment of heat during the sliding wear. However, at higher thermal energy of 1.440 KJ/mm the CoF slightly increased with value of 0.58 compared to CoF obtained at 0.7680 KJ/mm with value of 0.43, which is caused by a lower hardness and low concentration of SiC particles, as discussed earlier. This phenomenon caused more friction on the surface and finally increased the CoF value of the sample.

By evaluating the properties simultaneously between wear rate and COF, it can be observed that the performance of tribological resistance is improved by increasing the thermal energy at the maximum setting of 0.768 KJ/mm. Appropriate thermal energy has generally increased the

deposition and compatibility between SiC particles and DSS to produce complete melting of dissolved SiC and eventually improve the hardness and tribological properties.

### 3.4 Worn Surface Analysis

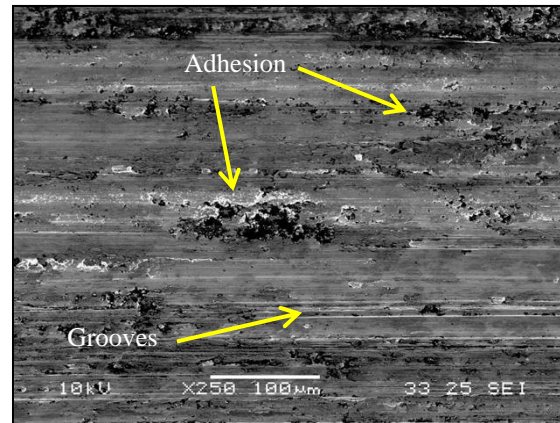
The wear characteristics of the surface modified DSS were analyzed from the SEM images taken at magnification of 250X after the wear test and illustrated in Figure 8. The worn surface for the surface modified DSS with lower thermal energy of 0.480 KJ/mm exhibited ploughing compared to higher thermal energy as shown in Figure 8(a). In this case, less concentration of SiC in this sample promotes the detachment of the substrate material during rubbing, hence produces a deep groove.

For the sample with 0.768 KJ/mm and 1.440 KJ/mm, the intensity of the scratch mark on the worn surface was reduced with the formation of mild and moderate striation. Further, highly concentrated SiC particles in the modified layer with thermal energy of 0.768 KJ/mm enable to resist the abrasion by the alumina ceramic ball and restrained the wear rate. As evident it can be seen only shallow grooves and less abrasive wear compared to other samples as shown in Figure 8(b). At this condition, as the blending and compatibility of SiC particles with the substrate material augmented, and a stronger modified layer formed and reasonably induced load during the wear test. However, at thermal energy of 1.440 KJ/mm as shown in Figure 8(c), it reveals the formation of slight grooves and moderate striation due to low concentration of SiC and hardness in this sample.

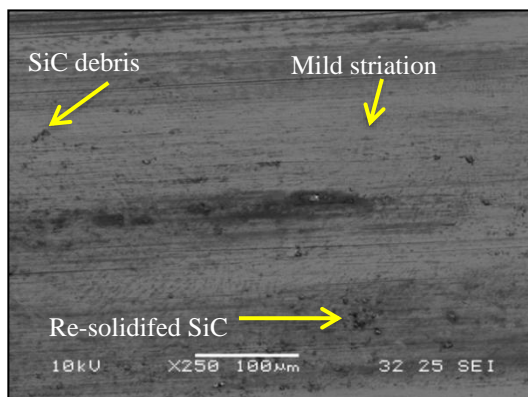
Note that because of the high heat in the wear test and the oxygen in the surrounding air, oxidizing chemicals and the mechanism of oxidative wear may occur in all samples. When oxygen is present, the two surfaces that are in contact react to the surrounding environment, separating the surface layers from the surface as particles. By combining oxygen with the surface layer of the sample, a ceramic layer is created that acts as a self-lubricating layer as the wear continues. Heat produced during friction accelerates oxidation (Kheradmand et al. 2022).

## CONCLUSIONS

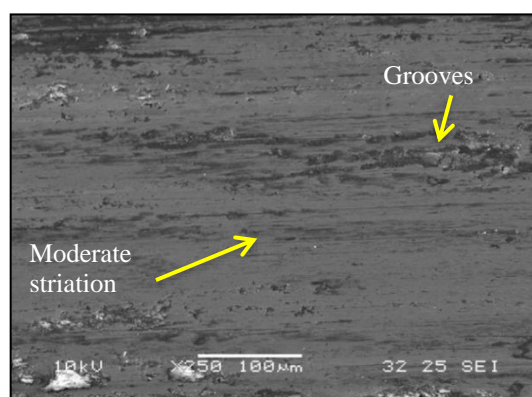
- a) It has been successfully accomplished to surface alloy the AISI Duplex-2205 by incorporating 60  $\mu\text{m}$  SiC particles and melting it using TIG torch procedures. For surface alloyed DSS to be of the highest quality, thermal input is crucial. From this investigation, the following findings can be made.
- b) The thermal energy between 0.48 KJ/mm and 0.768 KJ/mm has produced a smooth surface without any defects. However, some pores and cracks were observed with thermal energy of 1.440 KJ/mm due to high fluidity melt and slow cooling.
- c) In comparison to the untreated DSS, which had a hardness of 250 Hv, the surface modified DSS had a maximum hardness of 1245 Hv due to the complete dissolved of SiC producing the dendritic microstructure, which was reached with a heat input of 0.768 kJ/mm.
- d) The best thermal energy obtained was 0.768 KJ/mm that resulted in the lowest wear rate of  $3.0 \times 10^{-4} \text{ mm}^3/\text{Nm}$  and friction coefficient of 0.43.



(a)



(b)



(c)

Figure 8: SEM images of the wear ball on disc of surface modified DSS fabricated under thermal energy of (a) 0.48 KJ/mm, (b) 0.768 KJ/mm and (c) 1.440 KJ/mm.

## ACKNOWLEDGEMENTS

The financial support for this research was provided by FRGS/1/2023/TK10/UTEM/02/1 and FRGS/1/2023/FTKIP/F00554. Authors also are grateful to Universiti Teknikal Malaysia Melaka for the support that made this study possible.

## REFERENCES

- Adeleke, S. and Maleque M.A. (2016). TIG Melted Surface Modified Titanium Alloy for Cylinder Liner Application. *International Journal of Automotive Engineering and Technologies*, 4(3), 130-138.
- Adeleke, S.A. and Maleque, M.A. (2014). Tungsten Inert Gas Surface Alloying of Commercial Purity Titanium (CP-Ti) with Fe-C-Si Ternary Mixtures. *Advanced Materials Research*, 1024, 207-210.
- Amuda, M.O.H., & S. Mridha. (2011). Effect of Energy Input on Microstructure and Hardness of TIG Welded AISI 430- Ferritic Stainless Steel. *Advanced Materials Research*, 264-265, 390-396.

- Azwan, M., Maleque, M. A. and Rahman, M. M. (2019). TIG torch surfacing of metallic materials - a critical review. *Trans. Inst. Metal Finish.* 97, 12-21.
- Bello, K. A., Maleque, M. A., Adebisi, A. A., & Dube, A. (2016). Preparation and characterisation of TIG-alloyed hybrid composite coatings for high-temperature tribological applications. *Transactions of the IMF*, 94(4), 211–221.
- Bello, K. A., Maleque, Md. Abdul and Adebisi, Adetayo A. (2020). Processing of Ceramic Composite Coating via TIG Torch Welding Technique. *Encyclopedia of Renewable and Sustainable Materials*, 4, 523–535.
- Bharadwaj, V., Rai, A.K., Upadhyaya, B.N., Singh, R., Rai, S.K. & Bindra, K.S. (2022). A study on effect of heat input on mode of welding, microstructure and mechanical strength in pulsed laser welding of Zr-2.5 wt.%Nb alloy. *Journal of Nuclear Materials*, 564, 153685.
- Guo, N., Hu, H., Tang, X., Ma, X., & Wang, X. (2023). The Effect of TIG Welding Heat Input on the Deformation of a Thin Bending Plate and Its Weld Zone. *Coatings*, 13, 2008.
- Idriss, A. N. M., Kasolang, S., Maleque M.A., Ramdziah Md Nasir, Nasir, M. N. (2021). An overview on the importance of surface modification by TIG and lasers incorporating carbides and their relations to wear behaviours. *Jurnal Tribologi*, 29, 96-116.
- Kheradmand, A.B., Fattahi, M.R., Tayebi, M., Hamawandi, B. (2022). Tribological Characterization of Reinforced Fe Matrix Composites with Hybrid Reinforcement of C, Cu, and SiC Particulates. *Crystals*, 12, 598.
- Kumar, S. & Kumar, A. (2022). Wear resistance and hardness properties of TiB<sub>2</sub>- Fe coating developed on AISI 1020 steel by tungsten inert gas (TIG) cladding. *Ceramic International*, 48, 30052 – 30065.
- Kumar, S. & Singh, A.P. (2024). Characterization of surface properties of TiC ceramic coating developed on AISI 1020 steel. *Surfaces and Interfaces*, 48, 103960.
- Liu, H., Lv, S.; Xuan, Y., Oliveira, J.P., Schell, N., Shen, J., Deng, J., Wang, Y. & Yang, J. (2023). Effects of Heat Input on Weld Microstructure and Properties in Keyhole TIG Welding of Invar 36 Alloy. *Materials*, 16, 3692.
- Mamat, M.F, Hamzah, E., Ibrahim, Z, Rohah A.M. and Bahador, A. (2015). Effect of Filler Metals on the Microstructures and Mechanical Properties of Dissimilar Low Carbon Steel and 316L Stainless Steel Welded Joints, *Materials Science Forum*, 819, 57-62
- Mridha, S. and Dyuti, S. (2011). Effects of Processing Parameters on Microstructures and Properties of TIG Melted Surface Layer of Steel. *Advanced Materials Research*, 264-265, 1421 – 1426.
- Mridha, S. (2005). Titanium nitride layer formation by TIG surface melting in a reactive environment. *Journal of Materials Processing Technology*, 168, 471–477.
- Moi, S.M., Pal, P. K., Bandyopadhyay, A., & Rudrapati, R. (2019). Effect of Heat Input on the Mechanical and Metallurgical Characteristics of TIG Welded Joints. *Journal of Mechanical Engineering*, 16(2), 29-40.
- Muñoz-Escalona, Sillars, P., Marrocco, F., Edgar, T., Mridha, S. & Baker, T.N. (2020). Silicon carbide particulates incorporated into microalloyed steel surface using TIG: microstructure and properties, *Materials Science and Technology*, 36, 17-32.
- Oleiwi, A.A. and Abdul Sameea Jasim Jilabi, A.S.J. (2024). The Effects of travel speed of tungsten inert gas cladding of tungsten carbide and nickel composites on the microstructure of stainless steel, *Advances in Science and Technology Research Journal*, 18(4), 177–190.

- Paijan, L.H., Mamat, M.F., Abu Bakar, M.H, and Abd Aziz, M.S. (2024). Influence of Thermal Input on Microstructure and Wear Properties of Surface Alloyed DSS with SiC by TIG Melting Techniques, *Malaysian Journal of Microscopy*, 20(1), 123-133.
- Paijan, L. H., Maleque, M.A. (2018). Tribological properties of surface coated duplex stainless steel containing SiC ceramic particles *Jurnal Tribologi*, 18, 136-148.
- Paraye, N.K., Ghosh, P.K. and Das, S. (2021). Surface modification via in situ formation of titanium carbide in ferrous matrix through TIG arcing. *Material Letters*, 283, 128723.
- Ren, X., Zou, H., Diao, Q., Wang, C., Wang, Y., Li, H., Sui, T., Lin, B. & Yan, S., (2023). Surface modification technologies for enhancing the tribological properties of cemented carbides: A review. *Tribology International*, 180, 108257.
- Sahoo, C.K., Masanta, M. (2018). Microstructure and wear characteristic of hard and wear resistance TiC coating deposited on aluminium by tungsten inert gas (TIG) cladding process. *J Braz. Soc. Mech. Sci. Eng.* 40, 247.
- Subramaniam, S., Nithyaprakash R., Abbas G., Pramanik A., Basak, A. K. (2021). Tribological behavior of silicon nitride-based ceramics - A review, *Jurnal Tribologi* 29, 57-71.
- Yuvaraj, N. (2018). Surface Composite Fabrication through TIG arc Process: A Review. *International Journal of Emerging Technologies in Engineering Research (IJETER)*, 6(5), 59-62.